Plasma resonance in anisotropic layered high-T_c superconductors

Shigeki Sakai
Electrotechnical Laboratory, Umezono, Tsukuba, Ibaraki 305-8568, Japan

N. F. Pedersen
Department of Electric Power Engineering, Technical University of Denmark, DK-2800 Lyngby, Denmark
(Received 21 December 1998; revised manuscript received 19 May 1999)

The plasma resonance is described theoretically by the inductive coupling model for a large stacked Josephson-junction system such as the intrinsic Josephson-junction array in anisotropic high-T_c superconductors. Eigenmodes of the plasma oscillation are analytically described and a numerical example for the large stack case $N=50$ is given. The scaling length characteristic of each mode is discussed. Numerical results for the plasma resonance for $N=50$ in the presence of an external rf drive with wave number k are given. For k different from zero possible resonance modes among the eigen oscillation modes are shown, and it is further demonstrated that for $k=0$ the resonance takes place as a collection of N independent resonant Josephson junctions. Some guidelines for possible experiments are shown. It is also shown that very recent microwave experiments for the plasma resonance can be explained by this theory based on the inductive coupling, and collective longitudinal plasma oscillations are discussed. [S0163-1829(99)06637-0]

I. INTRODUCTION

There has recently been considerable interest in stacked Josephson junctions. For the case of low-T_c superconductors, the stacks can be formed, for example, by layers of $(Nb/AlO_x/)_nNb$.[1] For anisotropic layered high-T_c superconductors such as $Bi_2Sr_2CaCu_2O_x$ (BSCCO) and $Tl_2Ba_2Ca_2Cu_3O_x$ (TBCCO) it has been demonstrated that the crystal itself shows the features of stacked Josephson junctions, in this case often referred to as intrinsic Josephson-junction stacks.[2]

An interesting case occurs when the thickness t of the superconducting (S) layer is comparable to or less than the magnetic penetration depth λ_L, of the S layer. In such cases strong inductive coupling[3,4] can be expected among the Josephson junctions making the stack. In the case of a $(Nb/AlO_x/)_nNb$ stack, λ_L is about 90 nm, and thus the condition of $t<\lambda_L$ can be realized easily.[5] For the case of BSCCO intrinsic Josephson-junction stacks, λ_L is of the order of 100 nm while t is about 0.3 nm, i.e., only a few atomic layers thick.[2] Since $t \ll \lambda_L$, the inductive coupling is extremely strong.

Some major important phenomena of this system are the Josephson plasma resonances,[6–8] and the flux flow or fluxon dynamics[5,9] that can be described by the inductive coupling mechanism. As for the plasma resonance, we have recently presented the analytical formalism and shown some selected results, in particular for the case where the stack number N is small.[10]

In this paper, we theoretically describe the plasma resonance for the case of large $N(\gg 1)$ in order to focus on the correct understanding of the plasma oscillation in anisotropic high-T_c superconductors. Since the formalism is general, the theory can be used also for low-T_c stacked Josephson junctions. In Sec. II, the stacked junction system is described by the inductive coupling model by introducing a compact vector-matrix formalism. The description follows the previously published theory with respect to the inductive coupling model,[3] except that a more general expression for the external current bias terms is introduced. Next, the analytic form for plasma oscillations is presented, also using the compact vector-matrix notation and the results for some special cases are discussed. In Sec. III, eigenmodes of the plasma oscillation are analytically described and a numerical example for the large stack case $N=50$ is given. The scaling length characteristic of each mode is discussed. In Sec. IV, numerical results of the plasma resonance for $N=50$, in the presence of an external rf drive with wave number k are given. For k different from zero possible resonance modes among the eigen oscillation modes are shown, and it is further demonstrated that for $k=0$ the resonance takes place as a collection of N independent resonant Josephson junctions. In Sec. V we first show some guidelines for possible experiments, and also discuss collective longitudinal plasma oscillations. Such oscillations have been discussed by several authors in the framework of the charge coupling mechanism.[11–13]

II. THEORETICAL MODEL

A. System description

We first review briefly the theory of superconducting multilayers (stacked Josephson junctions) by Sakai, Bodin, and Pedersen,[3] based on inductive coupling through the superconducting layers. For convenience here the results are given in a compact vector-matrix form and by using parameters of the single barrier Josephson junction such as the Josephson penetration length, the plasma frequency, and the quasiparticle loss parameters. By using these parameters the plasma resonance phenomena characteristic of stacked Josephson junctions can be understood more easily. Although the analysis in the later sections is based on the assumption of identical layers and junctions, the formalism for general cases is presented here, because it will be valuable not only for a

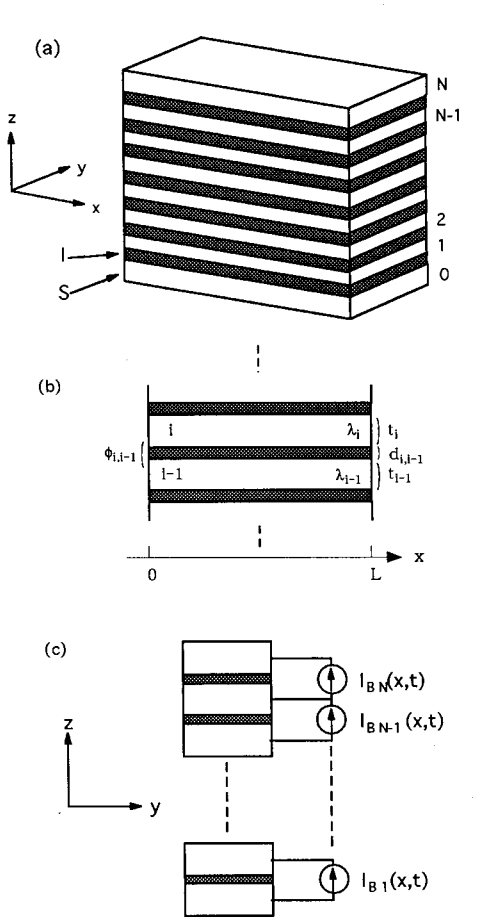

FIG. 1. (a) Schematic picture of a vertically N-stacked Josephson junction. (b) Enlarged diagram showing the parameter notation for convenience. (c) A stacked junction system with a bias current set.

system having parameter fluctuations but also for intrinsic Josephson junctions modulated by advanced atomic-layer control technology.

The system of N-stacked Josephson junction (schematically shown in Fig. 1) can be expressed as[3]

$$\Lambda_J^2 \frac{\partial^2 \vec{\phi}}{\partial x^2} = \mathbf{D}(\vec{Q} - \mathbf{J}^{-1}\vec{I}_B), \tag{1}$$

where $\vec{\phi}$, $\vec{Q}$, and $\vec{I}_B$ are the column vectors whose ith components are the phase difference ϕ_{ii-1}, dimensionless junction current Q_{ii-1}, and the bias current $I_{B,ii-1}$, of the ith Josephson junction, respectively: Q_{ii-1} is the sum of the supercurrent, displacement current, and quasiparticle tunnel current.

$$Q_{ii-1} = \frac{1}{\omega_{ii-1}^2}\frac{\partial^2 \phi_{ii-1}}{\partial t^2} + \frac{\alpha_{ii-1}}{\omega_{ii-1}}\frac{\partial \phi_{ii-1}}{\partial t} + \sin\phi_{ii-1}. \tag{2}$$

$\omega_{ii-1} = (2eJ_{ii-1}/\hbar C_{ii-1})^{1/2}$ is the ith junction maximum plasma frequency, the meaning of which will be discussed later, and $\alpha_{ii-1} = (\hbar/2eJ_{ii-1}C_{ii-1})^{1/2}G_{ii-1}$ is the well-known dimensionless loss parameter, where C_{ii-1}, G_{ii-1}, and J_{ii-1} are the capacitance, quasiparticle tunnel conductance, and the maximum supercurrent of the ith junction, respectively.

The bias current $I_{B,ii-1}$ can be a function of x and t. The simplest case of $I_{B,10} = I_{B,21} = \cdots = I_{B,NN-1} (= I_B)$ corresponds to the bias current I_B entering from the top (Nth) superconducting layer and leaving through the bottom (0th) layer. In this paper we will hereafter assume this simplest case.

D is a tridiagonal matrix including the inductive coupling mechanism. The nonzero elements are the unity diagonal elements ($D_{ii} = 1$) and the nearest-neighbor elements ($D_{ii\pm1} \equiv) S_{ii\pm1}$ that express the coupling strength:

$$\begin{aligned} S_{ii-1} &= \frac{s_{i-1}}{d'_{ii-1}} \cdot \frac{J_{i-1i-2}}{J_{ii-1}} \\ S_{ii+1} &= \frac{s_i}{d'_{ii-1}} \cdot \frac{J_{i+1i}}{J_{ii-1}} \end{aligned}, \tag{3}$$

where

$$d'_{ii-1} = d_{ii-1} + \lambda_{i-1}\coth\left(\frac{t_{i-1}}{\lambda_{i-1}}\right) + \lambda_i \coth\left(\frac{t_i}{\lambda_i}\right), \tag{4a}$$

$$s_i = -\frac{\lambda_i}{\sinh\left(\frac{t_i}{\lambda_i}\right)}. \tag{4b}$$

As shown in Fig. 1(b), d_{ii-1} is the insulating layer thickness of the ith junction, and t_i and λ_i are the thickness and magnetic penetration length of the ith superconducting layer. Λ_J and **J** are the diagonal matrices whose ith element are the so-called Josephson penetration length, $\lambda_{ii-1} = (\hbar/2e\mu_0 d'_{ii-1}J_{ii-1})^{1/2}$, and the maximum supercurrent J_{ii-1} of the ith junction, respectively. Note the difference between λ_{ii-1} and λ_i. The former is the Josephson penetration length of the ith junction, and the latter is the London penetration depth of the ith superconducting layer. Using this vector-matrix notation the boundary conditions at both edges ($x = 0, L$) in a uniform magnetic field H_a along the y direction are

$$\left[\frac{\partial \vec{\phi}}{\partial x}\right]_{x=0,L} = -\Lambda_J^{-2}\mathbf{D}\mathbf{J}^{-1}\vec{I}H_a, \tag{5}$$

where $\vec{I}$ is the column vector, all elements of which are unity.

Two special cases of the system described by Eq. (1) are:

(i) The case where the inductive coupling is zero, i.e., $s_i = 0$ in Eq. (4b). Then the coupling matrix **D** becomes the diagonal unit matrix. The whole matrix in Eq. (1) becomes diagonal, and the system is simply the collection of N-independent Josephson junctions,

$$\lambda_{ii-1}^2\frac{\partial^2 \phi_{ii-1}}{\partial x^2} = \frac{1}{\omega_{ii-1}^2}\frac{\partial^2 \phi_{ii-1}}{\partial t^2} + \frac{\alpha_{ii-1}}{\omega_{ii-1}}\frac{\partial \phi_{ii-1}}{\partial t} + \sin\phi_{ii-1} - \frac{I_B}{J_{ii-1}}, \tag{6}$$

for $i = 1,2,\ldots,N$. Thus in this case ω_{ii-1} is, in an exact sense, the plasma frequency of the ith junction, and the Josephson penetration length λ_{ii-1} defines the length scale of the ith junction.

(ii) The case where $\vec{\phi}$ is uniform in the x direction. Since the left-hand side of Eq. (1) is zero, it is evident that the system equations are decomposed to N independent Josephson-junction equations, in spite of the presence of the nonzero s_i terms,

$$\frac{1}{\omega_{ii-1}^2}\frac{\partial^2\phi_{ii-1}}{\partial t^2}+\frac{\alpha_{i,i-1}}{\omega_{ii-1}}\frac{\partial\phi}{\partial t}+\sin\phi_{ii-1}-\frac{I_B}{J_{ii-1}}=0, \quad (7)$$

for $i=1,2,\ldots,N$. This means that the inductive coupling takes place through the term $\partial^2\phi/\partial x^2$ as was also discussed in Ref. 10.

B. Analytic form for plasma oscillations

The plasma oscillation analysis follows the small signal expansion,[10,14] and the bias current $I_B=I_{\rm dc}+I_{\rm rf}\cos(kx-\omega t)$ is assumed with $|I_{\rm rf}|\ll J_{ii-1}$ for any i. $I_{\rm dc}$ is set to be smaller than the smallest J_{ii-1} in N junctions. Correspondingly, $\vec{\phi}$ has two terms $\vec{\phi}=\vec{\phi}^{(0)}+\vec{\phi}^{(1)}$ with $\phi_{ii-1}^{(0)}=\arcsin(I_{\rm dc}/J_{ii-1})$. For mathematical convenience, $I_{\rm rf}\cos(kx-\omega t)$ is replaced with $(I_{\rm rf}/2)\exp[j(kx-\omega t)]$, where $j^2=-1$. The real physical quantity can then be obtained as a sum of the solutions for this case and its complex-conjugate case. Then the solution of the time-dependent small-signal term $\phi^{(1)}$ has the form $\vec{\phi}^{(1)}=\vec{A}\exp[j(kx-\omega t)]$, and $\vec{A}$ can be obtained by solving

$$\{k^2\Lambda_J^2-\mathbf{DP}(\omega)\}\vec{A}=\mathbf{DJ}^{-1}\vec{I}\frac{I_{\rm rf}}{2}. \quad (8)$$

Here $\mathbf{P}(\omega)$ is a diagonal matrix, where the ith diagonal element P_{ii-1} is expressed as

$$P_{ii-1}=\left(\frac{\omega}{\omega_{ii-1}}\right)^2-\cos\phi_{ii-1}^{(0)}+j\alpha_{ii-1}\left(\frac{\omega}{\omega_{ii-1}}\right). \quad (9)$$

Let us here confirm that Eq. (8) also has the same properties as those discussed in Sec. II A.

(i) In the case that the inductive coupling is zero, **D** becomes diagonal. All matrices are diagonal and thus we obtain the uncoupled solutions, $A_{ii-1}=I_{\rm rf}/\{2(k^2\lambda_{ii-1}^2-P_{ii-1})J_{ii-1}\}$, for $i=1,2,\ldots,N$. This means that the plasma resonance for the ith junction takes place if k and ω of the external rf bias term exist on the plasma dispersion curve, $(k\lambda_{ii-1})^2=(\omega/\omega_{ii-1})^2-\cos\phi^{(0)}$.

(ii) In the case that the rf bias term is uniform along x, i.e., $k=0$, the coupling matrix **D** can be eliminated from both the left- and right-hand side of Eq. (8), and we obtain N uncoupled solutions, $A_{ii-1}=-I_{\rm rf}/(2P_{ii-1}J_{ii-1})$. This means that if the rf frequency ω coincides with the ith junction plasma frequency $\omega_{ii-1}\cdot(\cos\phi_{ii-1}^{(0)})^{1/2}$, the resonance appears by the inductive coupling mechanism even in the case when excited uniformly along x.

Furthermore, it should be remarked that if there is no external rf bias, $I_{\rm rf}=0$, Eq. (8) defines the eigen oscillation modes of the system by solving

$$det\{k^2\Lambda_J^2-\mathbf{D}P(\omega)\}=0. \quad (10)$$

In the final part of this section we give an explicit form in the case where all junctions and layers are identical. Then unnecessary subscripts can be dropped, e.g., $S\equiv S_{ii\pm1}=s/d'$, $J\equiv J_{ii-1}$, and $P\equiv P_{ii-1}$, and new notations are defined as $\lambda_J\equiv\lambda_{ii-1}$. In that case Eq. (8) becomes

$$\begin{pmatrix} k^2\lambda_J^2-P & -SP & 0 & \cdots \\ -SP & k^2\lambda_J^2-P & \ddots & \ddots \\ 0 & \ddots & \ddots & \\ \vdots & \ddots & & \end{pmatrix}\begin{pmatrix} A_{10} \\ A_{21} \\ \vdots \\ \vdots \end{pmatrix} = \frac{I_{\rm rf}}{2J}\begin{pmatrix} 1+S \\ 1+2S \\ \vdots \\ \vdots \end{pmatrix}. \quad (11)$$

III. ANALYSIS OF EIGEN OSCILLATION MODES

In this and the next section, the case where the stack has all identical layers and junctions will be treated. The eigenmodes of the system is obtained by solving Eq. (11) with the right-hand side equal to zero, and neglecting the loss terms.

The results show that an N junction stack has N eigenmodes. For the mth mode, the k-ω plasma dispersion relation becomes

$$\left(\frac{\omega}{\omega_p}\right)^2=1+[k\lambda_m^{(N)}]^2, \quad (12)$$

where $\omega_p=\omega_{po}\sqrt{\cos\phi^{(0)}}$ with $\omega_{po}=(2eJ/\hbar C)^{1/2}$, and

$$\lambda_m^{(N)}=\frac{\lambda_J}{\sqrt{\cos\phi^{(0)}}}\cdot\left[1-2S\cos\left(\frac{m\pi}{N+1}\right)\right]^{-1/2}. \quad (13)$$

The asymptotic velocity $c_m^{(N)}$ when $\omega\gg\omega_p$ (and also $k\lambda_m^{(N)}\gg1$) is $c_m^{(N)}=\omega_p\lambda_m^{(N)}$. The corresponding eigen vector of the mth mode is given by

$$A_{ii-1}^m=\sqrt{\frac{1}{N+1}}\sin\left[\frac{i(N+1-m)\pi}{N+1}\right], \quad \text{for } i=1,2,\ldots,N. \quad (14)$$

Equation (12) means that if ω and k in the mth mode are normalized to ω_p and $(\lambda_m^{(N)})^{-1}$, all plasma dispersion curves for $m=1,2,\ldots,N$ are identical. It also means that a good scaling factor of k in the mth mode is $\lambda_m^{(N)}$, in other words, the spatial scaling factor along x depends on the mode excited.

By recalling the definition of S ($S<0$), we find, from Eq. (13), $\lambda_m^{(N)}\geqslant\lambda_J/\sqrt{\cos\phi^{(0)}}$ for $m\geqslant(N+1)/2$, and $\lambda_m^{(N)}<\lambda_J/\sqrt{\cos\phi^{(0)}}$ for $m<(N+1)/2$. In particular, in the limit of $N\gg1$

$$\left.\begin{matrix}\lambda_N^{(N)} \\ \lambda_1^{(N)}\end{matrix}\right\}=\frac{\lambda_J}{\sqrt{\cos\phi^{(0)}}}\cdot\frac{1}{\sqrt{1\pm2S}}. \quad (15)$$

Furthermore, if we consider the limit of $t/\lambda_L\ll1$ where $\lambda_L=\lambda_i$ for $i=1,2,\ldots,N$, then we get

$$\lambda_N^{(N)}=\left(\frac{\hbar}{2e\mu_0(d+t)J\cos\phi^{(0)}}\right)^{1/2} \quad (16a)$$

and

$$\lambda_1^{(N)}=\left(\frac{\hbar}{2e\mu_0 J\cos\phi^{(0)}(2\lambda_L)}\right)^{1/2}\left(\frac{t}{2\lambda_L}\right)^{1/2} \tag{16b}$$

with $c_N^{(N)}=[\mu_0 C(d+t)]^{-1/2}$. Note that $d+t$ in Eq. (16) is the interlayer spacing, and in this limit $\lambda_N^{(N)}\equiv\lambda_c$ where λ_c is the characteristic distance often used in the literature.[11,12] The plasma dispersion relation [Eq. (12)] is expressed, using this scaling length λ_c, as

$$\left(\frac{\omega}{\omega_P}\right)^2=1+\left(\frac{\lambda_m^{(N)}}{\lambda_N^{(N)}}\right)^2(k\lambda_c)^2. \tag{17}$$

Note that the Nth mode in an N stack is always an all in-phase mode and the $N=1$ mode is always an antiphase mode, i.e., a mode where the ac phase polarity is always opposite between any neighboring two junctions. This is evident by inserting $m=N$ and $m=1$ into Eq. (14). Thus the relevant scaling length of all in-phase modes is $\lambda_N^{(N)}(=\lambda_c)$ and that of the antiphase mode is $\lambda_1^{(N)}$.

Using typical parameters for $Bi_2Sr_2CaCu_2O_x$ intrinsic Josephson junctions, $d=1.2$ nm, $t=0.3$ nm, $\lambda_L=200$ nm, we have $1+2S=4.5\times10^{-6}$ and the plasma dispersion curves for the case $N=50$ are shown in Fig. 2(a), where the scaling length for the all in-phase mode λ_c is used [see Eq. (17)]. At a given k, Fig. 2(a) predicts the possibility of not only the plasma resonance at the in-phase mode ($m=50$) but also may other resonance from $m=1-49$. Most of the curves in Fig. 2(a), typically from $m=1-40$, are condensed into one zone where ω is rather independent of $k\lambda_c$. In other words, under the scaling length λ_c, the plasma frequency of these curves are very insensitive to the variation of k.

It should be pointed out that the curves not belonging to the above-mentioned zone (typically from $m=45-49$) are independent of N in the limit of $N\gg1$ and in the very strong coupling limit, meaning that $|S|$ is less than but very close to 0.5. In such case, and when $m=N$, or m is very close to N but less than N,

$$\frac{\lambda_m^{(N)}}{\lambda_N^{(N)}}=\frac{c_m^{(N)}}{c_N^{(N)}}=\frac{1}{N+1-m}. \tag{18}$$

In this limit, $\lambda_N^{(N)}$ and $c_N^{(N)}$ themselves, as shown in Eq. (16), are independent of N, and the ratio in Eq. (18) does not depend on N. That is $\lambda_m^{(N)}/\lambda_N^{(N)}=c_m^{(N)}/c_N^{(N)}=\frac{1}{2},\frac{1}{3},\frac{1}{4},\ \ldots$ for $m=N-1,N-2,N-3,\ \ldots$, respectively.

IV. PLASMA RESONANCE ANALYSIS

The plasma resonance for large N cases is discussed by solving Eq. (11). Figure 2(b) shows the frequency dependence of the resonance intensity for $N=50$ and $k=0.2\cdot\sqrt{\cos\phi^{(0)}}/\lambda_J$. We assume the loss parameter $\alpha/\sqrt{\cos\phi^{(0)}}=0.01$. The voltage appearing per junction in the plasma analysis is smaller than the voltage jump (20–30 mV) per junction, and thus the chosen value of the loss parameter is not unrealistic from the estimation of conductances in such cases for BSCCO intrinsic Josephson junction.[15] The resonance intensity is evaluated by $\Sigma_i|A_{ii-1}|/N$.

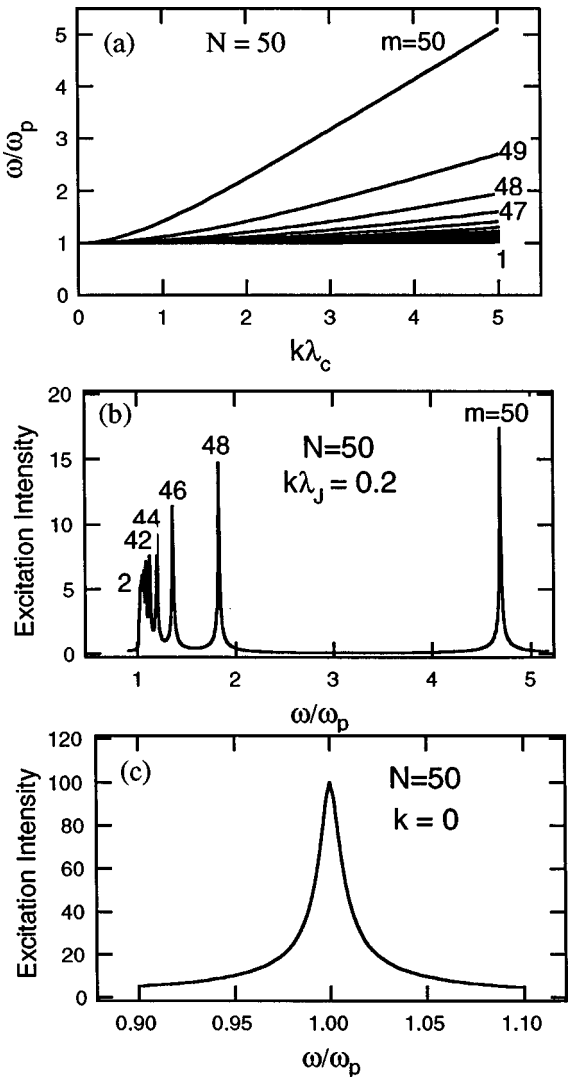

FIG. 2. (a) Plasma dispersion relation curves for $N=50$. Used parameters are $d=1.2$ nm, $t=0.3$ nm, and $\lambda_L=200$ nm. λ_c is the scaling length of the all in-phase mode $m=N$. (b) and (c) Frequency dependence of the resonance intensities at (b) $k=0.2\cdot\sqrt{\cos\phi^{(0)}}/\lambda_J$ and (c) $k=0$. $\alpha/\sqrt{\cos\phi^{(0)}}=0.01$ is assumed. The resonance intensity was evaluated by $\Sigma_i|A_{ii-1}|/N$.

In Fig. 2(b), we find a lot of resonance peaks as predicted in the previous section. The peak with the largest frequency corresponds to the all in-phase mode ($m=50$). The second and third largest resonance frequencies are almost $\frac{1}{3}$ and $\frac{1}{5}$ times as large as the largest one, respectively. As is evident from Eq. (18), the resonance at these frequencies corresponds to the modes at $m=48$ and 46.

We find that every second mode obtained by counting m downwards from the all in-phase mode ($m=N$) gives a resonance. This confirms the discussion in Ref. 10. The reason for this rule may be understood from the relationship between the form of the solution and the bias configuration. Let us, for example, see the solutions of the top and bottom junctions for the m mode. From Eq. (14) we have $A_{NN-1}^m=\pm A_{10}^m$ where ''+'' and ''−'' should be chosen when $(N-m)$ is the even or odd, respectively. $A_{NN-1}^m=A_{10}^m$ is a resonance case because it fits to the configuration of the external rf bias.

Figure 2(c) shows the result for $k=0$. The same param-

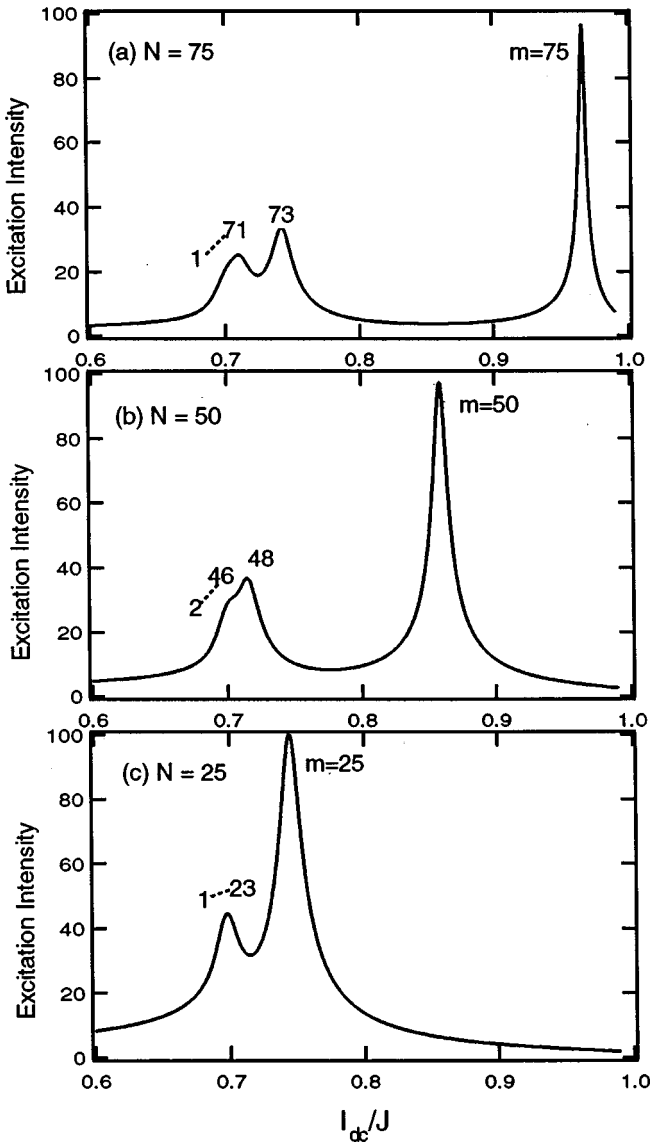

FIG. 3. Bias current dependence of the resonance intensity. For calculation, $\omega/\omega_{po}=0.85$, $k\lambda_J=0.02$, $\alpha=0.01$, and $1+2S=4.5\times10^{-6}$ were assumed. (a) $N=75$, (b) $N=50$, and (c) $N=25$. The peak position at the $m=N$ mode strongly depends on the stacked junction number N. The lower number mode peaks are merged together, and its position is insensitive to N.

eters as in the case of Fig. 2(b), except for $k=0$, were used. We find only one peak at $\omega=\omega_p$ which may be understood from the plasma dispersion curve of Fig. 2(a). $k=0$ means that the oscillation is uniform along the x direction. According to the inductive coupling model, the coupling takes place through the term $\partial^2\phi/\partial x^2$; in this case, with $k=0$, the second derivative vanishes and the plasma oscillation takes place independently in each junction. Note, however, that Fig. 2(c) is the result of summing the same plasma oscillation of all junctions. This is not any evidence of phase coherent motion but is a simple mathematical trick, since the parameters of all the junctions are identical. If the parameters deviate from each other, the resonance frequency and the phase motion of the individual junctions are shifted from each other, and thus oscillation phases between neighboring

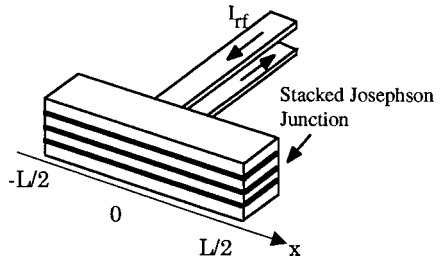

FIG. 4. Experimental configuration demonstrating that the bias current forms a standing wave. Since the Fourier components have forms of $\cos(kx-\omega x)+\cos(kx+\omega x)$, the analysis in the present paper can be used directly.

junctions are independent. This is also clear in connection with the discussion in a paragraph between Eqs. (9) and (10).

V. DISCUSSIONS

A. Guideline to possible experiments

It is not always easy to sweep the frequency widely in experiments using waveguides. Instead, since ω_p in Eq. (12) is a function of $\cos\phi^{(0)}$, I_{dc} can be conveniently used to change the ratio (ω/ω_p).

By using I_{dc} instead of $\cos\phi^{(0)}$ in Eq. (12), the plasma dispersion curve of the m th mode is explicitly expressed by I_{dc}:

$$\frac{I_{dc}}{I}=\left\{1-\left[\left(\frac{\omega}{\omega_p}\right)^2-\left(\frac{c_m^{(N)}}{c_0}\right)^2(k\lambda_J)^2\right]^2\right\}^{1/2} \tag{19}$$

with $c_0=(\mu_0 d' C)^{-1/2}$. Thus by fixing ω and k and varying I_{dc}, the plasma resonance peaks can be traced. Figure 3 shows a numerical result. $\omega/\omega_{po}=0.85$, $k\lambda_J=0.02$, $\alpha=0.01$, and $1+2S=4.5\times10^{-6}$ were assumed. Figures 3(a), (b), and (c) are the result for $N=75$, $N=50$, and $N=25$, respectively. Again, every second mode can resonate. An experimentally good evidence may be that the peak position at the $m=N$ mode strongly depends on the stacked junction number N. On the other hand, the lower number mode peaks are merged together, and its position is very insensitive to N, in general agreement with the previous discussion.

In the plasma resonance analysis we assumed that the rf bias current has a traveling wave form $I_{rf}\cos(kx-\omega t)$. Let us discuss how spatially dependent I_{rf} bias can be attained. In general—at least if a ground plane is not used—there will be a nonhomogeneous current distribution with spikes at the edges of the electrodes.[16] This will give rise to current and voltages in the stack, which has a fundamental spatial component defined by the length of the junction in the x direction. Another intentionally designed example is shown in Fig. 4, where the bias electrode size is much smaller than x direction length L. The bias in the stack has a maximum at $x=0$, and decreases with $|x|$ increasing. Thus the bias forms a standing wave. Its Fourier components have forms of $\cos(kx-\omega t)+\cos(kx+\omega t)$. Therefore the analysis in the present paper can be used directly.

B. Collective longitudinal plasma oscillation

The so-called longitudinal plasma excitation has been discussed by several authors (Refs. 11–13) in the framework of

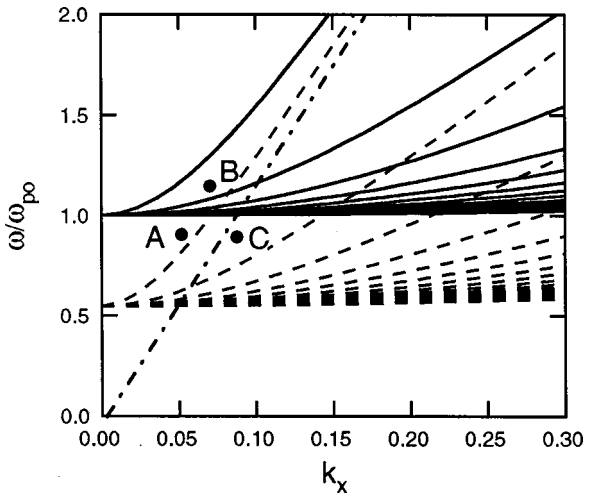

FIG. 5. Schematic graph showing relationship between the plasma dispersion curves and the k-ω conditions. A set of solid curves is the dispersion of possible eigenmodes at $B_{dc}=0$, and a set of dashed curves is the dispersion when B_{dc} is some nonzero value. The all in-phase mode dispersion approaches asymptotically to the dash-dot line in the figure with much increasing ω/ω_{po}, regardless of the B_{dc} magnitude.

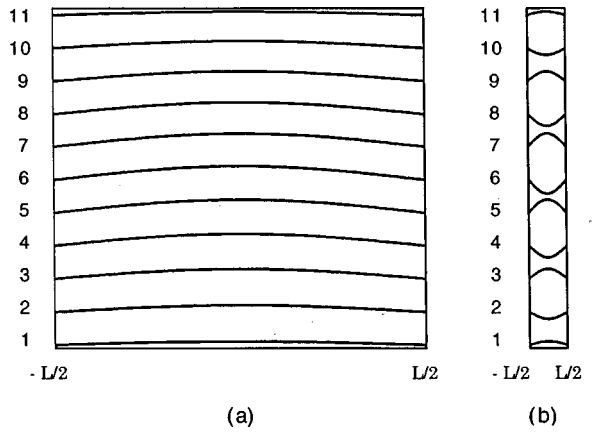

FIG. 6. Schematic snapshot of $\partial\vec{\phi}^{(1)}/\partial x$ as a function of x for explaining the scaling and the longitudinal mode. (a) all in-phase mode; (b) antiphase mode. The sample size L for the all in-phase mode should be large because its large scaling length $\lambda_N^{(N)}$ is large. Under the same driving frequency, L for the antiphase mode should be small because of the small $\lambda_1^{(N)}$. From the figures the excitation patterns are found to vary not only with x but also with z, in other words, the resonance is longitudinal.

the theory based on the charge coupling through the superconducting layers. Here it is shown that the inductive coupling theory we are proposing can explain the experimental observations.

Kadowaki *et al.* in Ref. 12 and Kakeya *et al.* in Ref. 13 have investigated sample size dependence of plasma resonance in single crystalline $Bi_2Sr_2CaCu_2O_x$ and discussed the observed resonance modes. In order to adjust the plasma frequency to a fixed frequency in experiments, they applied and slowly changed a static magnetic field B_{dc} parallel to the c axis of BSCCO instead of changing the bias current.[6–8,12,13]

In the case that the microwave electric field was applied in the direction parallel to the BSCCO c axis ($E_{rf}\|c$), the resonance frequency was almost constant for the change of the sample size L_x from 0.8–1.8 mm where L_x is the sample size in the ab plane (Refs. 12 and 13). Their interpretation is that, probably due to this very weak L_x dependence, the resonance mode was the longitudinal plasma mode by the charging effect model[11] in which k_z vs ω dispersion is very weakly dependent on k_z.[12,13]

Since $L_x \ll \lambda_g/2$ where λ_g is the fundamental wavelength in their cavity box size, the excited plasma is mostly uniform in the samples along x, i.e., $k_x \sim 0$. Therefore we can interpret this as simple gathering of $k_x=0$ plasma excitation by N independent Josephson junctions as was shown in Fig. 2(c). This means that these experimental results can be explained by the inductive coupling model and do not always necessitate introducing the charging effect model in Ref. 11.

In the case that the microwave magnetic field was applied in parallel to the ab plane of BSCCO ($H_{rf}\|ab$), Kadowaki *et al.* observed one peak with showing a strong L_x dependence of the plasma resonance.[12] Kakeya *et al.* showed resonance with two peaks.[13] The first peak has very weak L_x dependence of the resonance frequency and the second has large dependence, and in their text they also suggested multipeak observation more than two peaks in a large L_x case.[13]

In order to interpret this, the authors in Ref. 13 assume the continuous medium in the z direction [Eqs. (6)–(8) in Ref. 13], and inevitably the excitation electric field E_z is uniform along z. This may correspond to the in-phase motion in the discrete model in the present paper. As a consequence of their model, however, they do not consider other excitation modes besides the uniform excitation along z. By using the discrete stacked junction model with the inductive coupling that results in the presence of multiple plasma resonance modes, the phenomena under $H_{rf}\|ab$ could be explained.

The reason why the peak number of the resonance in the experiment of $H_{rf}\|ab$ was changed is understood by the relationship between the dispersion curves and the experimental conditions that is shown in Fig. 5. There are many cases, depending on experimental k and ω conditions. With increasing static magnetic field B_{dc} in the c direction, plasma dispersion curves are moved downwards. In the figure the curves are shown by dashed lines and solid lines, respectively, according to the conditions with and without B_{dc}. If a point in the k-ω coordinate decided by the experimental frequency and the sample cavity size is located on the region (like A in Fig. 5) lower than all dispersion curves when $B_{dc}=0$, the first peak appearing with the increase of B_{dc} may correspond to the dispersion curves condensed into one zone that is very insensitive to k_x, and the second and higher peaks are sensitive to k_z. If the point is set to be like B in Fig. 5, the peak corresponding to the condensed zone cannot be observed and observable peaks are sensitive to k_x (the sample size L_x). If the point is located on the right side area of the asymptotic straight line for the all in-phase mode whose gradient is the velocity $c_N^{(N)}$ (like C in Fig. 5), the resonance of the all in-phase mode never appears during these B_{dc} sweeping experiments.

Finally, we further discuss the scaling and the longitudinal mode. As an extreme case we compare the highest velocity (all in-phase) mode and the lowest velocity mode (antiphase mode between adjacent junctions). Since the scaling length is expressed as Eq. (13), if the experimental frequency

is fixed, k is small and L_x is large for the highest velocity mode meaning that the sample cavity size should be designed to be large. For the lowest velocity mode the situation is opposite. A schematic picture is shown in Fig. 6. If L_x is fixed, the frequency for the fundamental excitation becomes large and small for the highest and lowest velocity modes, respectively. As is clear from Fig. 6, the excitation is longitudinal. The excitation wavelength along z is of the order of the interlayer spacing $d+t$ in the case of Fig. 6(b). In the case of the inductive coupling model, therefore, plasma excitation modes for $k \neq 0$ are inevitably longitudinal. There has been similar discussion by Kleiner with respect to the Fiske eigenmode.[17]

VI. CONCLUSION

Plasma resonance in anisotropic layered high-T_c superconductors has been described theoretically by the inductive coupling mechanism. An N junction stack has N plasma eigenmodes. Each mode has a scaling length along x, i.e., in the ab plane. For example, the difference in this length between the in-phase mode of all the junctions ($m=N$) and the antiphase mode of adjacent two junctions ($m=1$) is quite large. If the k-ω dispersion curves of these eigenmodes are shown using the scaling length of the all in-phase mode, most of the curves become very insensitive to the change of k and are condensed into one zone. An actual calculation with an rf driving term for $N=50$, using BSCCO parameters, has demonstrated that multiple resonances may appear with changing the frequency. Every second mode obtained by counting m downwards from the all in-phase mode ($m=N$) gives a resonance, that is explained by the symmetric properties of the modes and the rf bias configuration. The calculation has also shown that even for the $k=0$ case the plasma resonance appears as a simple gathering of N independent Josephson junctions. As a guideline for possible experiments a method of sweeping the dc bias current instead of tuning the frequency has been discussed; this predicts a strong stack size (N) dependence of the resonance of the all in-phase mode. A comparison of the theory with very recent microwave experiments of the plasma resonance has been made. The experimental results of the dependence of the resonance position on the sample dimension in the x direction (for both $E_{\mathrm{rf}} \| c$ and $H_{\mathrm{rf}} \| ab$ cases) have been well explained within the theory by the inductive coupling model described in this paper. It has also shown that for the $k \neq 0$ cases, the excitation waves inevitably have longitudinal wave component along z as well as the component along x.

[1] H. Kohlstedt, F. Konig, P. Henne, N. Thyssen, and P. Caputo, J. Appl. Phys. **80**, 5512 (1996).

[2] R. Kleiner and P. Müller, Phys. Rev. B **49**, 1327 (1994).

[3] S. Sakai, P. Bodin, and N. F. Pedersen, J. Appl. Phys. **73**, 2411 (1993).

[4] S. Sakai, A. V. Ustinov, H. Kohlstedt, A. Petraglia, and N. F. Pedersen, Phys. Rev. B **50**, 12 905 (1994).

[5] A. V. Ustinov and H. Kohlstedt, Phys. Rev. B **54**, 6111 (1996).

[6] Ophelia K. C. Tsui, N. P. Ong, Y. Matsuda, Y. F. Yan, and J. B. Peterson, Phys. Rev. Lett. **73**, 724 (1994); Ophelia K. C. Tsui, N. P. Ong, and J. B. Peterson, *ibid.* **76**, 819 (1996).

[7] Y. Matsuda, M. B. Gaifullin, K. Kumagai, K. Kadowaki, and T. Mochiku, Phys. Rev. Lett. **75**, 4512 (1995); Y. Matsuda, M. B. Gaifullin, K. Kumagai, M. Kosugi, and K. Hirata, *ibid.* **78**, 1972 (1997).

[8] L. N. Bulaevskii, M. Zamora, D. Baeriswyl, H. Beck, and J. R. Clem, Phys. Rev. B **50**, 12 831 (1994).

[9] G. Hechtfischer, R. Kleiner, K. Schlenga, W. Walkenhorst, P. Müller, and H. L. Johonson, Phys. Rev. B **55**, 14 638 (1997).

[10] N. F. Pedersen and S. Sakai, Phys. Rev. B **58**, 2820 (1998).

[11] M. Tachiki, T. Koyama, and S. Takahashi, Phys. Rev. B **50**, 7065 (1994); in *Coherence in High Temperature Superconductors*, edited by G. Deutsher and A. Revcolevschi (World Scientific, Singapore, 1996), p. 371; T. Koyama and M. Tachiki, Phys. Rev. B **54**, 16 183 (1996).

[12] K. Kadowaki, I. Kakeya, M. B. Gaifullin, T. Mochiku, S. Takahashi, T. Koyama, and M. Tachiki, Phys. Rev. B **56**, 5617 (1997).

[13] I. Kakeya, K. Kindo, K. Kadawaki, S. Takahashi, and T. Mochiku, Phys. Rev. B **57**, 3108 (1998).

[14] N. F. Pedersen, M. R. Samuelsen, and K. Saermark, J. Appl. Phys. **44**, 5120 (1973).

[15] K. Schlenga, R. Kleiner, G. Hechtfischer, M. Mössle, S. Schmitt, P. Müller, Ch. Helm, Ch. Preis, F. Forsthofer, J. Keller, H. L. Jonson, M. Veith, and E. Steinbeiss, Phys. Rev. B **57**, 14 158 (1998).

[16] See, for example, T. Van Duzer and C. W. Turner, in *Principles of Superconductive Devices and Circuits* (Edward Arnold, London, 1981), p. 107.

[17] R. Kleiner, Phys. Rev. B **50**, 6919 (1994).